

VELOCITY IMAGING SYSTEM FOR DETECTION OF MOVING SCATTERERS

Necmi Serkan Tezel
e-mail: necmi@ehb.itu.edu.tr

N.Gökhan Kasapoğlu
e-mail: gokhan@ehb.itu.edu.tr

Bingül Yazgan
e-mail: yazgan@ehb.itu.edu.tr

Istanbul Technical University, Electrical-Electronics Faculty, Electronics & Communication Engineering Department
80626, Maslak, Istanbul, Turkey

Key words: VSAR ,deblurring ,velocity imaging

ABSTRACT

Conventional synthetic aperture radar systems is not convenient for targets whose scatterers have different motion. If scatters' motion has a radial component, it will displace along the azimuth direction in its SAR image. This effect is not important for targets whose scatters has same radial component such as ship and plane imaging, because of same displacement. But in ocean imaging this will cause blurring effect. In this study, we applied velocity synthetic aperture radar (VSAR) [6] imaging algorithm for point scatterers whose position and radial velocity are different.

I. INTRODUCTION

Synthetic aperture radar (SAR) are designed to obtain an image of the reflectivity of an observed area. Conventional SAR systems are not designed to measure surface motion , such as ocean imaging applications. That motion causes a distortion of the SAR image. We show capable of the VSAR imaging algorithm such as providing velocity map and compensating azimuth displacements for moving point scatterers. VSAR imaging algorithm provides to estimate the velocities of the scatters in every range/azimuth cell. Knowledge of these velocities makes it possible to undo the velocity blurring and approximately reconstruct the reflectivity image. In addition to creating a deblurred SAR image, the VSAR system provides an estimate of the radial velocities of the dominant scatters. Thus, it can generate a velocity map of the observed area.

II. VSAR IMAGING MODEL

The VSAR system consists of M conventional SAR system located on the same platform, and a single transmitting element. (figure 1)

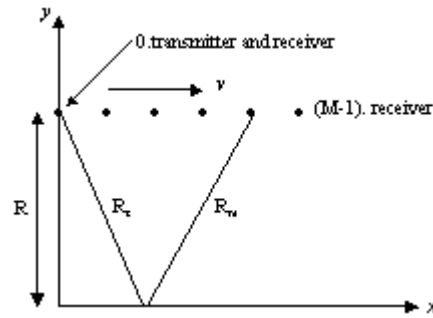


Figure 1 Bistatic SAR configuration

The returns from each transmitted pulse are received by all of the antenna elements and are processed coherently to produce a set of complex images. $Y_m(x,y)$ (where x and y are the azimuth and ground range coordinates). This SAR image formation step involves conventional processing:

Despite a conventional SAR processor would form the absolute value of the complex image at the last step, the VSAR processor uses the individual SAR images in their complex form. Clearly, the M complex SAR images have the same absolute value, but different phases. The phases contain the information about the velocity distribution along the azimuth strip. The main function of the VSAR processor is to extract velocity distribution from M complex SAR images. The set of complex SAR images $\{Y_m(x,y), m=0,...,M-1\}$ undergoes a post processing step, which brings out the velocity dimension. if we consider a set of image $\{Y_m(x,y), m=0,...,M-1\}$ as a single three dimensional image $Y(x,y,m)$ then this processing stage is applied along the m axis of the image. The resulting three dimensional image is the azimuth/range/velocity image of the observed scene. Finally, each 'velocity plane' is shifted by an amount proportional to its velocity, to correct for the motion induced azimuth displacement, and all the planes are added up to produce undistorted VSAR image.

The information contained in the set of velocity images can be presented in two different ways, One way is a

composite image obtained by direct pixel by pixel summation of the magnitudes of all the velocity images. The result is a deblurred version of a conventional SAR image. Another way is an image depicting the dominant velocity in each pixel. This image provides a velocity map of the observed area

Figure 2 shows the geometry of the VSAR scenario and illustrates the pertinent parameters. The azimuth and ground range coordinates are x and y , respectively. The flight altitude is H , V is the platform velocity, and t is time.

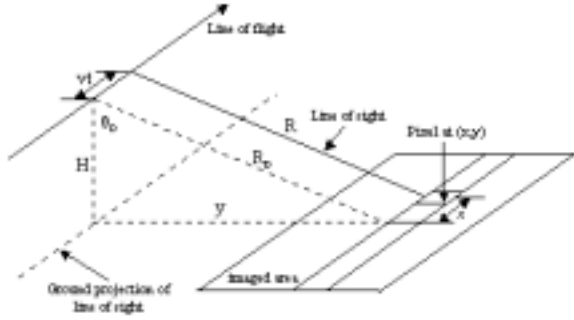


Figure 2 Geometry of VSAR scenario

If the instantaneous distance from the point $(x,y,z(x,t))$ to the m th receiver is $R(x,t,m)$ and assuming that the transmitter is collocated with zeroth receiver, the instantaneous phase of the signal received from this point by m th receiver

$$\phi(x, t, m) = \frac{2\pi[R(x, t, 0) + R(x, t, m)]}{\lambda} \quad (1)$$

The total signal at the m th receiver is,

$$s_m(t) = \int G(x)A(x, t)e^{j\phi(x, t, m)} dx \quad (2)$$

where range of integration is over the aperture of the real antenna, $G(x)$ is the two-way gain pattern and $A(x, t)$ is the complex reflectivity of the scatters.

The output of the m th SAR processor is

$$\begin{aligned} Y_m(\xi) &= \sum_{p=0}^{P-1} w_p^a s_m(t_p) e^{-j\phi_r(\xi, t_p, m)} \\ &= \sum_{p=0}^{P-1} w_p^a \int G(x)A(x, t_p) e^{j[\phi(x, t_p, m) - \phi_r(\xi, t_p, m)]} dx \end{aligned} \quad (3)$$

where $t_p = (2p+1)T/2P$, T being the integration time and P the number of the radar pulses. The sequence $\{w_p^a, 0 \leq p \leq P-1\}$ is an optional window (to be called the azimuth window), $\phi_r(\xi, t, m)$ is a phase reference function

and its aim to cancel the known terms in instantaneous phase (focusing) and the variable ξ represents the image azimuth coordinate.

The VSAR processor combines the individual SAR outputs as follows:

$$Z_q(\xi) = \sum_{m=0}^{M-1} w_m^v Y_m(\xi) \exp\left\{ \frac{j2\pi m(\xi - qn_v \Delta_x)}{n_v M \Delta_x} \right\} \quad (4)$$

where q is an integer in the range $[-M/2, M/2-1]$. The sequence w_m^v is an optional window. This operation is core of VSAR system. It extracts the velocity information from the M complex SAR images.

The final VSAR operation is to shift these images according to

$$Z_q^s(\xi) = Z(\xi + qn_v \Delta_x) \quad (5)$$

We call $Z_q^s(\xi)$ as velocity images. In order to interpret formula (5), consider the special case of a unit magnitude impulse scatter located at azimuth x_0 and having vertical velocity $v(x_0)$. The resulting $Z_q^s(\xi)$ is called the point-spread function (PSF) of the VSAR system and will give maximum response at $\xi = x_0$ and only specific q which depends its velocity. This means that scatters which have different velocity will be seen different images. This is why we call these images as velocity images.

The combined VSAR image is given by the sum of squares of the velocity images,

$$I(\xi) = \sum_{q=-M/2}^{M/2-1} Z_q^s(\xi) [Z_q^s(\xi)]^* \quad (6)$$

is a deblurred image of all scatters with all velocity.

III. SIMULATION : VSAR AND SAR IMAGES OF THE MOVING SCATTERERS

Let's assume that scatterers position and their velocity as follows:

In 5th pixel = 9m, stationary

In 9th pixel = 17m, 1m/s leaving from radar (-1m/s)

In 15th pixel = 29m, 0.5 m/s towards radar

And all the scatters are in the middle of the pixels.

Simulation parameter of the SAR system as follows:

Flight altitude of the platform : $H=2000$ m

Platform velocity : $V=250$ m/s

Pixel size: $\Delta_x=2$ m

Integration time : $T=0.1s$

Pulse repetition frequency : $PRF=1000\text{ Hz}$

Effectively integrated pulse number : $P=100$

Rectangular window and FFT in azimuth processing

Radar looking angle : $\theta_0=30^\circ$

Radar wavelength : $\lambda=1.5\text{ cm}$

Total number of the cross range pixels : $N=30$

Simulation parameters of the VSAR system as follows:

VSAR system contain multiple SAR systems so parameter of the VSAR system correspond same

parameter of the SAR system. In addition to above parameter;

Number of the antennas : $M=10$

Spacing between two adjacent antennas : $d=1.5\text{ m}$

Rectangular window and FFT in velocity processing

VSAR design parameter : $n_v=1$

When we make simulation, we get the results as follows:

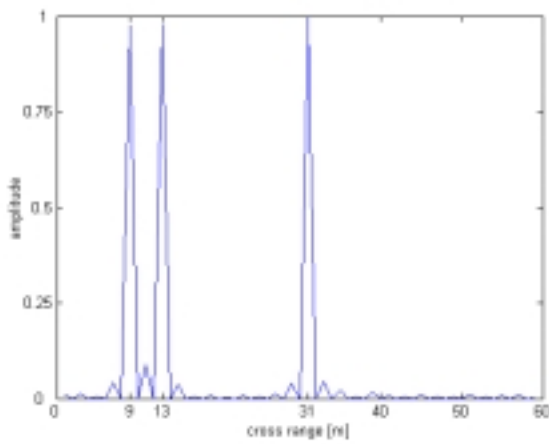


Figure 3 SAR image along the cross range

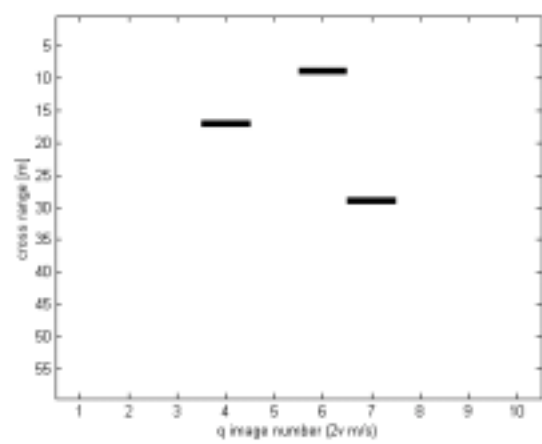


Figure 4 Velocity map of the observed area

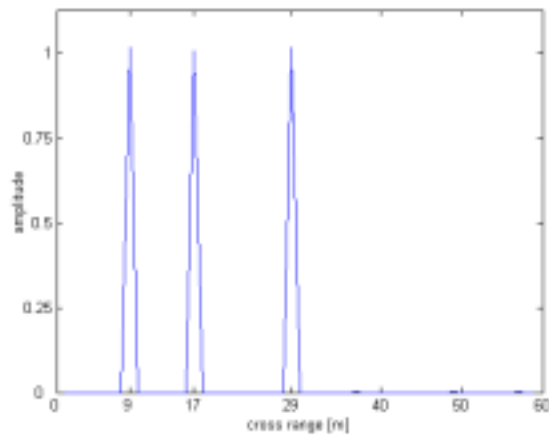


Figure 5 VSAR image along the cross range

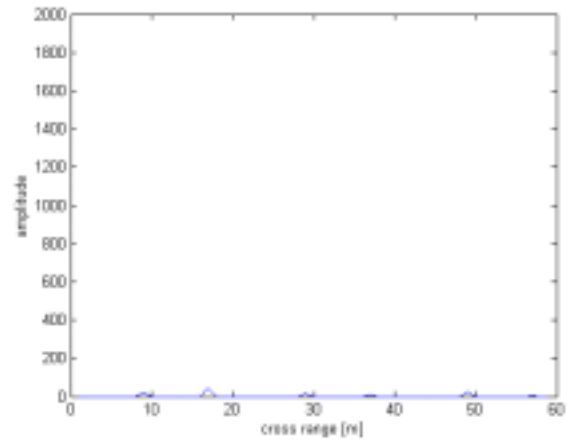


Figure 6 Image of the scatters whose velocity is -2.5 m/s

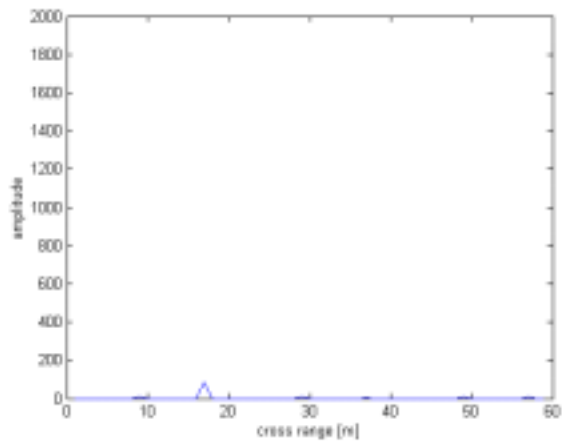


Figure 7 Image of the scatterers whose velocity is -2 m/s

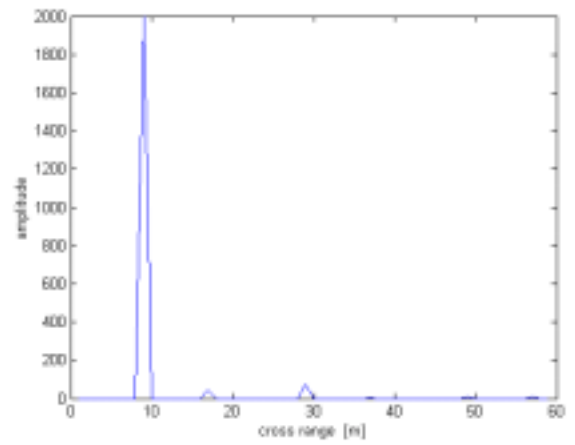


Figure 8 Image of the scatterers whose velocity is -0.5 m/s

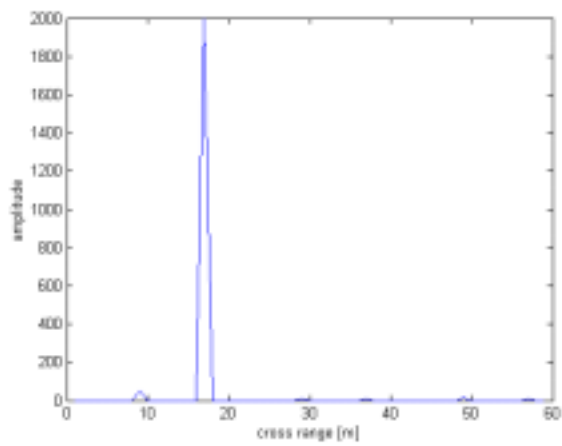


Figure 9 Image of the scatterers whose velocity is -1.5 m/s

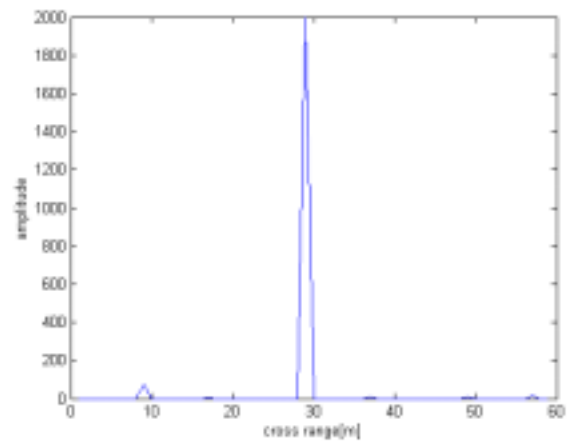


Figure 10 Image of the stationary scatterers

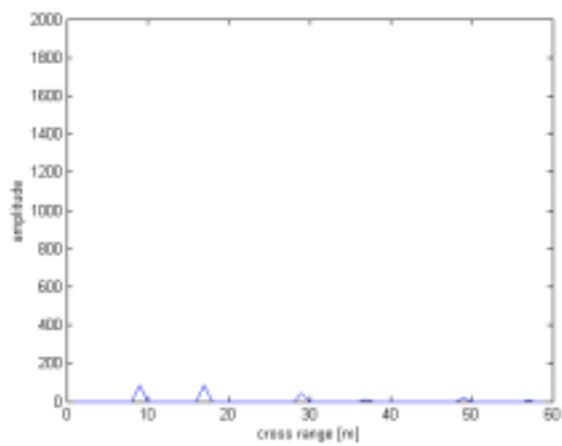


Figure 11 Image of the scatterers whose velocity is -1 m/s

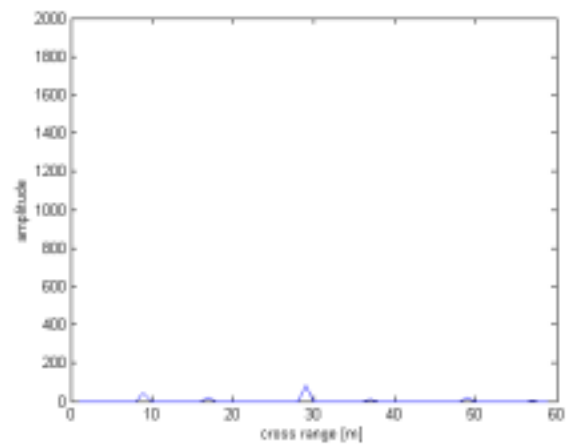


Figure 12 Image of the scatterers whose velocity is 0.5 m/s

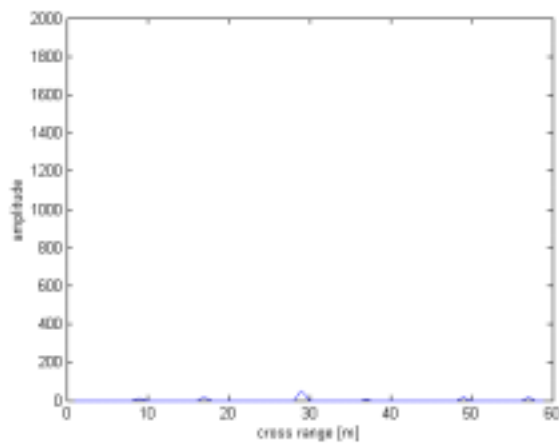


Figure 13 Image of the scatterers whose velocity is 1 m/s

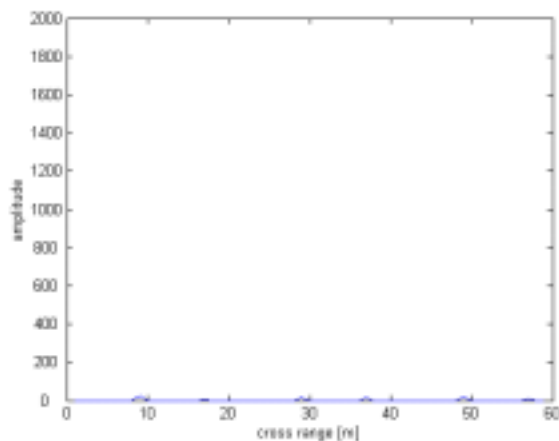


Figure 14 Image of the scatterers whose velocity is 1.5 m/s

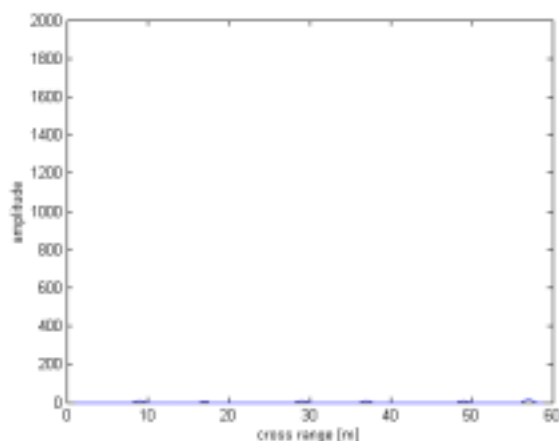


Figure 15 Image of the scatterers whose velocity is 2 m/s

IV.SIMULATION RESULTS

Although SAR image of the scatterers displaced along the cross range, because of their velocity (see fig 3), VSAR image of the scatterers placed to proper position (see fig 5) Velocity map of the observed area is shown in figure 4. Figures (6-15) shows velocity image of observed area whose scatterers' velocity are specific value.

V. CONCLUSIONS

In this study, we applied velocity SAR imaging algorithm for moving scatterers. Simulations demonstrated that, the VSAR imaging algorithm reduces the velocity blurring of the conventional SAR images, and provides velocity mapping of the observed area. However VSAR imaging algorithm requires larger amount of computations than conventional SAR imaging algorithm.

REFERENCES

- 1 Ender, J. 1993, Detectability of slowly moving targets using a multi-channel SAR with an along-track antenna array. In proceedings of SEE/IEE Conference SAR 93, Paris, May , 19-22
- 2 Ender, J. 1994 Signal processing for multi channel SAR applied to experimental SAR system AER. In Proceedings of the international radar conference (RADAR 94), Paris, May , 220-225
- 3 Ender, J. 1996 Detection and estimation of moving target signals by multi-channel SAR. AEU International Journal of Electronic Communication, 50,2 , 150-156
- 4 Ender, J. ,1996 The airborne experimental multi-channel SAR system AER-II. In Proceedings of EUSAR Mar.
- 5 Barbarossa, S. and Farina , A. 1994 Space-time-frequency processing of synthetic aperture radar signals. IEEE Transactions on Aerospace and Electronic Systems, 30, 2 , 341-358
- 6 Friedlander B., Porat B. A High Resolution Radar System for Ocean Imaging IEEE Transactions on Aerospace and Electronic Systems vol.34, No.3 July
- 7 Kasilingam, D.P.,and Shemdin, O.H. 1988 Theory of synthetic aperture imaging of the ocean surface Journal of Geophysical Research, 93, C11 Nov. , 13837-13848
- 8 Necmi Serkan Tezel Velocity Synthetic Aperture Radar for an ocean imaging MSc Thesis ITU Institute of Science and Technology.